Inorganic Chemistry

Article

pubs.acs.org/IC

Exchange Coupling Mediated by N−H···Cl Hydrogen Bonds: Experimental and Theoretical Study of the Frustrated Magnetic System in Bis(*o*-phenylenediamine)nickel(II) Chloride

Roger D. Willett,*[,†] Carlos J. Gómez-García,[‡] Brendan Twamley,[§] Silvia Gómez-Coca,[⊥] and Eliseo Ruiz[⊥]

[†]Department of Chemistry, Washington State University, Pullman, Washington 99164, United States

[‡]Instituto de Ciencia Molecular, Parque Científico, Universidad de Valencia, 46980 Paterna (Valencia), Spain

[§]University Research Office, University of Idaho, Moscow, Idaho 83844, United States

[⊥]Departament de Química Inorgànica and Institut de Recerca de Química Teòrica i Computacional (IQTCUB), Universitat de Barcelona, Diagonal 645, Barcelona 08028, Spain

Supporting Information

ABSTRACT: The title compound crystallizes in the monoclinic $P2_1/c$ space group with a = 11.2470(3) Å, b = 5.9034(2) Å, c = 12.0886(3) Å, β = 115.143(1)°, and V = 726.58(4) Å^3 and consists of discrete monomeric $NiCl_2$(o-phenylendiamine)$_2$ molecules. Each o-phen ligand coordinates in a bidentate mode with the chloride ions occupying *trans* positions in the resulting tetragonally distorted octahedral coordination sphere. Two discrete sets of N−H···Cl hydrogen bonds link the octahedral molecules into a two-dimensional network, with type 1 interactions linking adjacent monomers along the c axis and type 2 interactions linking monomers along the diagonals in the bc plane. Analysis of the magnetic data reveals the existence of weak antiferromagnetic coupling within the layers via these hydrogen bonds, in addition to the presence of zero field splitting, with the best fit obtained for a 1d antiferromagnetic model with g = 2.0917(7), J/k = −2.11(4) K [J = −1.47(3) cm^{-1}], and D = 1.05(3) cm^{-1} [$\beta = D/|J| = 0.72(6)$] for the model with $D > 0$ and g = 2.0911(6), J/k = −2.26(1) K [J = −1.57(1) cm^{-1}], and D = −0.86(1) cm^{-1} [$\beta = D/|J| = 0.55(6)$] for the model with $D < 0$. Theoretical calculations of the exchange coupling confirm the experimental results, yielding values of J_1 = −1.39 cm^{-1} for the type 1 hydrogen bonds and J_2/k = −0.56 cm^{-1} for the type 2 hydrogen bonds.

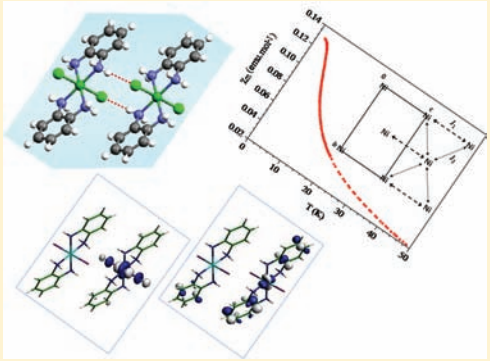

INTRODUCTION

The organic compound *o*-phenylenediamine is a well-known reagent that is used extensively in the preparation of Schiff base complexes.[1] The complex species obtained in solution with $NiCl_2$ is often used as a templating reagent in these syntheses.[2] In studies with metal ions, *o*-phenylenediamine has been shown to act in a variety of ways: as a bidentate ligand, as a monodentate ligand, and even as a bridging ligand.[3] On the other side, although Ni(II) complexes with *o*-cyclohexanediamine are quite numerous (up 27 examples can be found in the CCDC database updated Nov 2011),[4] the number of Ni(II) complexes with the corresponding aromatic *o*-phenylenediamine ligand is much lower (only seven complexes can be found in the CCDC database, including the title compound).[5,6] A preliminary report of the crystal structure of $NiCl_2$(*o*-phenylenediamine)$_2$ (henceforth $NiCl_2$(opda)$_2$) showed the structure contains discrete *trans* octahedral $NiCl_2$(opda)$_2$ species in which the *o*-phenylenediamine molecules serve as bidentate ligands.[6] In this paper, we reexamine the crystal structure of $NiCl_2$(opda)$_2$, focusing on the N−H···Cl hydrogen bond network, whose presence in this compound leads to an interesting example of molecular self-assembly through weak interactions, an important topic in supramolecular chemistry.[7] We report here the magnetic properties of the title compound, where octahedral Ni(II) complexes show weak antiferromagnetic interaction through the H-bonds. The fit of the magnetic properties to different 1D and 2D models with and without zero field splitting (ZFS) has raised an ambiguity with two possible exchange pathways. DFT calculations were performed to evaluate the magnetic coupling constant through the two different H-bond exchange pathways, since this methodology has proved to be a very useful tool to study the exchange interactions in dinuclear[8] or polynuclear complexes.[9]

EXPERIMENTAL SECTION

Crystal Growth and X-ray Analysis. X-ray intensity data were collected at 90(2) K using a Bruker/Siemens SMART APEX instrument (Mo Kα radiation, λ = 0.71073 Å) equipped with a Cryocool NeverIce low-temperature device. Data were measured using omega scans of 0.3° per frame for 5 s, and a full sphere of data was collected. A total of 2400 frames were collected with a final resolution

Received: April 6, 2012
Published: April 18, 2012

   dx.doi.org/10.1021/ic3007124 | *Inorg. Chem.* 2012, 51, 5487−5493

of 0.83 Å. Cell parameters were retrieved using SMART[10] software and refined using SAINTPlus[11] on all observed reflections. Data reduction and correction for *Lp* and decay were performed using the SAINTPlus software. Absorption corrections were applied using SADABS.[12] The structure was solved by direct methods and refined by a least-squares method on F^2 using the SHELXTL program package.[13] The structure was solved in the space group $P2_1/c$ by analysis of systematic absences. All non-hydrogen atoms were refined anisotropically. Data collection and refinement parameters are given in Table 1. Further details are provided in the Supporting Information. Crystallographic data for the structure has been deposited with the Cambridge Crystallographic Data Centre as supplementary publications no. CCDC-732815.

Table 1. Crystal Data and Structure Refinement

empirical formula	$C_{12}H_{16}Cl_2N_4Ni$
fw	345.90
T (K)	90(2)
cryst syst	monoclinic
space group	$P2_1/c$
a (Å)	11.2470(3)
b (Å)	5.9034(2)
c (Å)	12.0886(3)
β (deg)	115.143(1)
V (Å^3)	726.58(4)
Z	2
D_{calc} (Mg/m^3)	1.581
μ (mm^{-1})	1.694
F(000)	356
cryst size (mm^3)	0.38 × 0.14 × 0.13
cryst color and habit	blue needle
reflns collected	10 696
indep reflns	1674 [R(int) = 0.0157]
max. and min. transmn	0.8099 and 0.5654
data/restraints/params	1674/0/104
GOOF	1.070
final R indices [$I > 2\sigma(I)$]	R_1 = 0.0198, wR_2 = 0.0513
R indices (all data)	R_1 = 0.0204, wR_2 = 0.0518
largest diff peak and hole (e Å^{-3})	0.424 and −0.230

Magnetic Measurements. Variable-temperature susceptibility measurements were carried out in the temperature range 2−300 K with an applied magnetic field of 0.1 T on a ground polycrystalline sample (96.75 mg) with a SQUID magnetometer (Quantum Design MPMS-XL-5). The susceptibility data were corrected for the diamagnetic contributions of the sample as deduced by using Pascal's constant tables. In addition, the isothermal magnetization of the sample was measured at 2 K in fields ranging from 0 to 9 T with a Quantum Design PPMS-9 apparatus.

Computational Details. To support and validate the results of the magnetic study, theoretical calculations were undertaken for the exchange pathways present in this system. Since a detailed description of the computational strategy adopted in this work can be found elsewhere,[14−17] only a brief sketch of its most relevant aspects will be given here. A phenomenological Heisenberg Hamiltonian, $\hat{H} = -J\hat{S}_1\cdot\hat{S}_2$, is used to describe the exchange coupling in a dinuclear compound, where J is the exchange coupling constant and S_1 and S_2 the local spins on centers 1 and 2, respectively. It has been found that, when using DFT-based wave functions, a reasonable estimate of the exchange coupling constants can be obtained from the energy difference between the state with highest spin, E_{HS}, and the low-spin wave function, E_{LS} (traditionally called broken-symmetry solution) obtained by just flipping one of the spins through the following equation:

$$J = \frac{E_{LS} - E_{HS}}{2S_1S_2 + S_2} \quad (1)$$

This equation does not include the spin projection as originally proposed by Noodlemann et al.[18] The presence of the self-interaction error in the exchange−correlation functional includes an unspecified amount of nondynamic correlation energy, resulting in the fact that the monodeterminantal solution corresponding to the low-spin wave function provides an energy value close to that corresponding to the low-spin state.[14] The inclusion of the spin projection gives a strong overestimation of the calculated J values, especially for system with small S_i values.

The hybrid, DFT-based B3LYP method[19] has been used in all calculations as implemented in Gaussian03,[20] mixing the exact exchange with Becke's expression for the exchange functional[21] and using the Lee−Yang−Parr correlation functional.[22] The triple-ζ basis set proposed by Schaefer et al.[23] was employed including two extra p functions for the Ni atoms as well as a d polarization function and two s and p diffuse functions for Cl atoms in order to improve the description of the hydrogen bond interactions. Due to the small magnitude of the exchange coupling constants, all energy calculations must be performed including the *SCF* = *Tight* option of Gaussian to ensure sufficiently well converged values for the calculated energies.

RESULTS AND DISCUSSION

Structural Description. The monomeric *trans* octahedral $NiCl_2(opda)_2$ species, in which the *o*-phenylenediamine molecules serve as bidentate ligands, is illustrated in Figure 1.

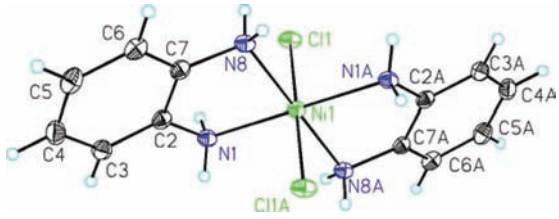

Figure 1. Illustration of the molecular structure for $NiCl_2$(*o*-phenylenediamine)$_2$.

Bond distances are normal (Ni−Cl = 2.4497(3) Å and Ni−N1 and Ni−N8 = 2.081(1) and 2.07(1) Å, respectively). The small bidentate bite angle (81.68(4)°) exerts a rhombic distortion on the tetragonally elongated octahedral coordination sphere. The octahedra are hydrogen bonded together into layers parallel to the *bc* plane through two sets of intermolecular hydrogen bonds, as illustrated in Figure 2. Pairs of N−H···Cl bonds (type 1) link adjacent octahedra along the *c* axis (N−Cl = 3.256 Å, Ni−Cl···N = 122.76°, H···Cl = 2.395 Å, and N−H···Cl = 171.98°), while single N−H···Cl bonds (type 2) (N−Cl = 3.275 Å, Ni−Cl···N = 144.46°, H···Cl = 2.417 Å, and N−H···Cl = 171.58°) link octahedra that lie at the unit cell corners and *bc* face centers. The structural parameters are virtually identical in both sets of hydrogen bonds, except for the Ni−Cl···N angles. Adjacent Ni/Cl hydrogen-bonded networks are separated by double layers of the phenyl groups of the *o*-phen ligands, as seen in the space-filling diagram in Figure 3. Adjacent layers are separated by unit cell translations in the *a* direction.

The analysis of the magnetic data (vide infra) shows that antiferromagnetic interactions are present in this system. These interactions must be mediated by the hydrogen bonds within the Ni/Cl layers. Via these hydrogen bond interactions, complex two-dimensional magnetic layers are defined. A number of possibilities exist, depending on the sign and magnitude of the exchange coupling via the two types of

dx.doi.org/10.1021/ic3007124 | Inorg. Chem. 2012, 51, 5487−5493

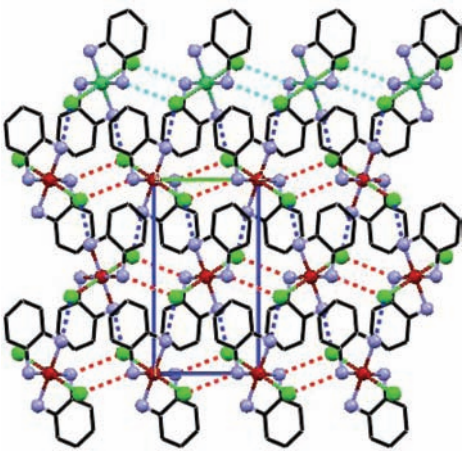

Figure 2. Illustration of the layer structure. Type 1 hydrogen bonds are shown as red, dashed lines, and type 2 as blue, dashed lines. Color code: Ni = red, Cl = green, N = blue. The *c* axis is horizontal, and the *b* axis is vertical.

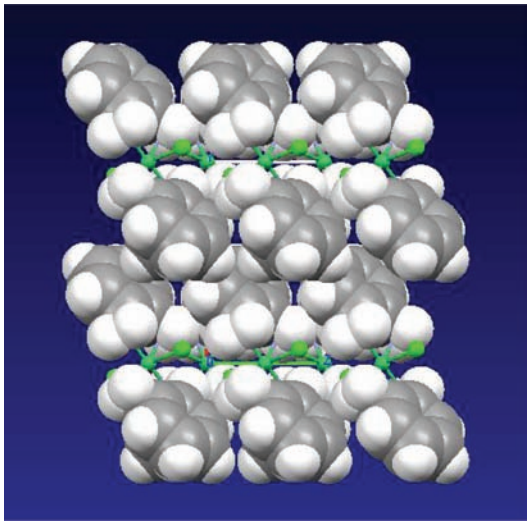

Figure 3. Space-filling illustration of the packing between layers, demonstrating the effective isolation of adjacent magnetic layers. The Ni and Cl atoms are shown as green balls.

hydrogen bonds. If the interactions through the pairs of hydrogen bonds along the *c* axis dominate (denoted as J_1), the $NiCl_2(opda)_2$ species will be linked into uniform one-dimensional magnetic chains (dashed lines in Scheme 1). In contrast, if the interactions through the single hydrogen bonds between the species at the cell corners and the *bc* face centers

Scheme 1

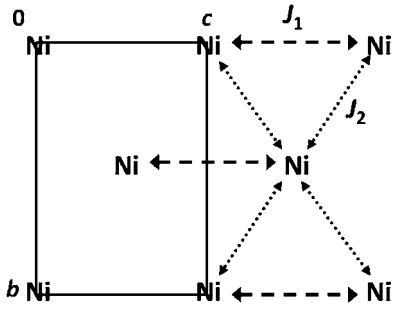

are dominant, denoted as J_2, they will link the system into a square magnetic lattice (dotted lines in Scheme 1). Importantly, it should be noted that if the J_1 interaction is antiferromagnetic, the coupling through the J_2 pathway will always be frustrated, be it ferromagnetic or antiferromagnetic, since the Ni ions in positions 0 and *c* present different spin orientation as J_1 is antiferromagnetic and the central Ni ion is equally coupled to both Ni ions (in 0 and *c* positions).

Magnetic Studies. To analyze the magnetic data, both zero field splitting in the $S = 1$ Ni(II) ions and the exchange coupling within the layers must be considered. The magnetic susceptibility data for the $NiCl_2(opda)_2$ sample show continuously increasing values as the temperature is lowered, as seen for the low-temperature portion of the data in Figure 4.

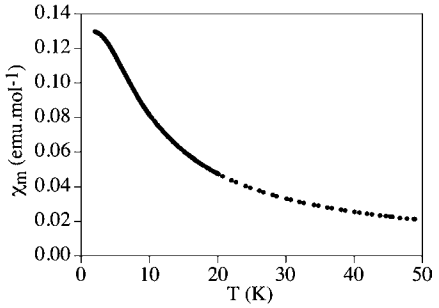

Figure 4. Low-temperature portion of the χ_m vs T plot.

At the lowest temperatures, there is just a hint that it is approaching a maximum value, suggesting the presence of dominant weak antiferromagnetic interactions within the layers. The plot of $\chi_m T$ vs T (Figure 5) shows continuously decreasing

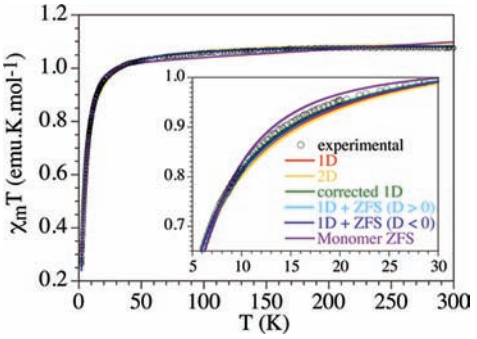

Figure 5. Plots of the experimental $\chi_m T$ vs T data (open circles) and theoretical calculations for a 1D, 2D, corrected 1D, monomer with ZFS, and 1D with ZFS for $D > 0$ and $D < 0$ models. Inset shows the low-temperature region.

values as the temperature is lowered, confirming the presence of dominant antiferromagnetic interactions. Although it could be argued that the decrease in the $\chi_m T$ product may be due *exclusively* to the presence of a zero field splitting in the $S = 1$ Ni(II) ions, the hint observed in the χ_m plot (Figure 4) and the fact that the decrease in the $\chi_m T$ product at low temperatures starts at ca. 50 K (Figure 5) suggest that there must be a dominant antiferromagnetic interaction (along with the ZFS, see below). The magnetization plot (M vs H, not shown) shows a value of ca. 1.6 μ_B at 9 T, below the expected value (ca. 2.0 μ_B), confirming the presence of dominant antiferromagnetic exchange interactions. As can also be seen in Figure 5, $\chi_m T$ is still declining rapidly at $T = 2$ K, with a $\chi_m T$ value less that 0.3

dx.doi.org/10.1021/ic3007124 | *Inorg. Chem.* 2012, 51, 5487−5493

emu K mol^{-1}. This result rules out the possibility that the system is behaving as a frustrated magnet.

According to the structural features described above, we can, in principle, imagine two possible limiting exchange pathways: (i) an $S = 1$ AFM 1D system[24] and (ii) an $S = 1$ AFM 2D system (quadratic layer antiferromagnet, QLAF).[25] These two models reproduce quite well the magnetic data in the whole temperature range with the following parameters: $J/k = -2.182(7)$ K [$J = -1.516(5)$ cm^{-1}] with $g = 2.095(1)$ for the 1D model and $J/k = -1.257(7)$ K [$J = -0.873(5)$ cm^{-1}] with $g = 2.099(1)$ for the 2D model (Figure 5 and Table 2).

Table 2. Magnetic Parameters Obtained with the Different Models Used (See Text)[a]

model	g	J (cm^{-1})	J' (cm^{-1})	$\|D\|$ (cm^{-1})
1D	2.095(1)	−1.516(5)		
corrected 1D	2.0877(5)	−1.72(1)	−0.22(1)	
2D	2.099(1)	−0.873(5)		
monomer ZFS	2.000(2)			12.0(1)
1D + ZFS ($D > 0$)	2.0917(7)	−1.47(3)		1.05(3)
1D + ZFS ($D < 0$)	2.0911(6)	−1.57(1)		−0.86(1)

[a]The Hamiltonian is written as $\hat{H} = -J\hat{S}_1 \cdot \hat{S}_2$.

Given the existence of two hydrogen-bonding pathways, the data were then fit to the molecular field corrected 1D model.[26] This model also reproduces quite well the magnetic data in the whole temperature range (Figure 5) with the following parameters: $J/k = -2.48(1)$ K [$J = -1.72(1)$ cm^{-1}] and $J'/k = -0.31(1)$ K [$J' = -0.22(1)$ cm^{-1}] with $g = 2.0877(5)$ (Table 2, the Hamiltonian is written as $\hat{H} = -J\hat{S}_1 \cdot \hat{S}_2$ in all cases). Because of the frustration induced by the J_2 pathway with J_1 being antiferromagnetic, the J' value corresponds to the overall local field and not directly with the J_2 pathway. Thus, it is impossible to assert the sign of the J_2 pathway from the analysis of the magnetic data. Thus, although the 1D model with the molecular field correction reproduces slightly better the magnetic data (especially at high temperatures), it can be argued that this fact may be only due to the increase in the number of fitting parameters (from two to three), and thus, the large number of adjustable parameters becomes an additional possible reason limiting the extraction of reliable exchange parameters in the fit. To summarize, we can conclude that there is a dominant weak antiferromagnetic interaction of ca. 1−2 cm^{-1} between the Ni(II) centers, in at least one direction, along with a possible ZFS.

Once having established the nature and approximate magnitude of the dominant magnetic coupling, we have tried to estimate the possible presence of a ZFS in the $S = 1$ Ni(II) ions using two different limiting models. In a first approach, we have assumed that the decrease in the $\chi_m T$ product is exclusively due to the presence of a ZFS, and accordingly, we have fit the magnetic properties with a simple $S = 1$ monomer with a ZFS.[26] This model gives only a rough agreement with $g = 2.000(2)$ and a $|D|$ value as high as 12.0(1) cm^{-1}. The relatively bad agreement and the high D value (usually below 6−8 cm^{-1} for Ni(II) ions)[27] confirm the need to consider an exchange coupling for the title compound. Thus, in a second approach, we have used the model including the ZFS proposed by Borrás-Almenar et al.[28] for an alternating antiferromagnetic $S = 1$ chain since this model can be reduced to a regular antiferromagnetic chain when the exchange alternation parameter (α) is fixed to 1 (unfortunately, there is no equivalent 2D AF model, including the ZFS, available). The two different expressions provided by this model (depending on the sign of the D parameter) give very good agreement with the experimental data over the whole temperature range with the following parameters: $g = 2.0917(7)$, $J/k = -2.11(4)$ K [$J = -1.47(3)$ cm^{-1}], and $D = 1.05(3)$ cm^{-1} [$\beta = D/|J| = 0.72(6)$] for the model with $D > 0$ and $g = 2.0911(6)$, $J/k = -2.26(1)$ K [$J = -1.57(1)$ cm^{-1}], and $D = -0.86(1)$ cm^{-1} [$\beta = D/|J| = 0.55(6)$] for the model with $D < 0$ (solid lines in Figure 5). Although both fits are very similar, precluding an unambiguous assignment of the sign of D, they confirm the coexistence of both contributions: a weak antiferromagnetic coupling and a ZFS. Note that the use of a molecular field corrected model for an AF $S = 1$ chain including a ZFS would simply increase to four the number of adjustable parameters but is not expected to significantly improve the fit.

Theoretical Results. Although the corrected 1D model suggests that the exchange pathways through the double hydrogen bonds along the c axis (type 1, J_1, Scheme 1) are more important than the single hydrogen bonds (type 2, J_2, Scheme 1), we cannot exclude the opposite possibility since the involved intermolecular distances are very similar in both cases. In addition, as noted above, the experimental magnetic data are not capable of predicting the sign of J_2. Therefore, in order to try to elucidate the correct magnetic coupling, we have performed calculations based on density functional theory (DFT) to evaluate the exchange coupling constants corresponding to the two interactions (types 1 and 2) as indicated in Figure 6. A brief description of the employed approach has been included in the Computational Details section. It is worth

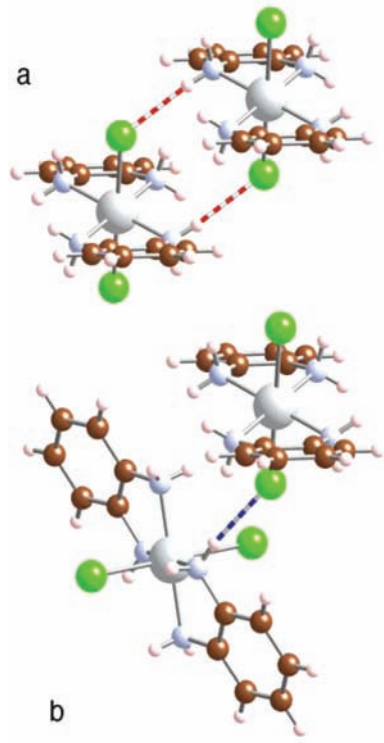

Figure 6. Representation of the two main intermolecular interactions. (a) Motif corresponding to the type 1 interaction (a double N−H···Cl bond with d(H···Cl) = 2.395 Å) in Figure 2; (b) type 2 interaction (a simple N−H···Cl bond with d(H···Cl) = 2.417 Å). Color code: Ni = gray, Cl = green, C = brown, and N = blue.

dx.doi.org/10.1021/ic3007124 | Inorg. Chem. 2012, 51, 5487−5493

noting that some theoretical studies devoted to the presence of the exchange pathways through intermolecular weak interactions have been performed by some of us[29,30] and other authors[31] with a remarkable accuracy in the estimation of the J values. Also, we would like to remark that this type of hydrogen bond involving N−H···Cl contacts plays a key role in some important complexes in molecular magnetism, such as the single molecule magnet Mn_4 dimer complex that exhibits exchange-biased quantum tunneling due to the presence of these weak interactions.[32]

The calculated J values corresponding to the two intermolecular exchange pathways represented in Figure 6 are −1.39 and −0.56 cm^{-1} for the type 1 and 2 bridges, respectively. These values are in agreement with the experimental data obtained from the fit of the magnetic properties (−1.72(1) and −0.22(1) cm^{-1} for the corrected 1D model, Table 2), confirming the presence of a weak antiferromagnetic interaction in both bridges. The relative strength of the two exchange pathways is basically related with the double pathway for the exchange present in the type 1 interaction since the H···Cl bond distances are very similar. To confirm this assumption, we have analyzed the influence of the H···Cl bond distance on the exchange interaction. The dependence of the J value for the type 1 model is represented in Figure 7, showing relatively small changes in the exchange

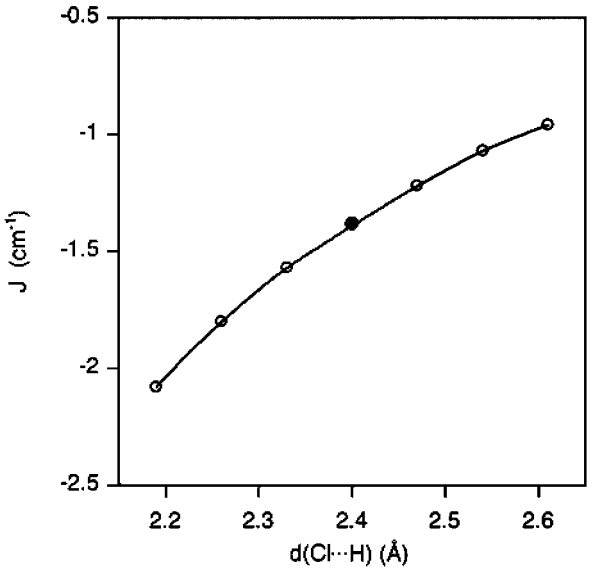

Figure 7. Dependence of the exchange coupling constant corresponding to the type 1 interaction on the intermolecular Cl···H bond distance calculated using the B3LYP functional. The solid black circle corresponds to the experimental bond distance in the studied compound.

interaction when the intermolecular distance is changed. Thus, the increase in the antiferromagnetic coupling due to a shortening of 0.2 Å in the H···Cl is less than 1 cm^{-1}. In order to complete the study of the influence of geometrical parameters, we performed a calculation of the type 2 structure, modifying the Ni−Cl···N angle (144.46°) until the value of 122.76°, corresponding to the type 1 interaction. The calculated J value (−0.28 cm^{-1}) shows a decrease of the exchange coupling constants because the spin delocalization of the Ni^{II} cation[33,34] on the axial chlorine atoms is mainly in the p orbitals (see Figure 8), and consequently, a smaller Ni−Cl···N

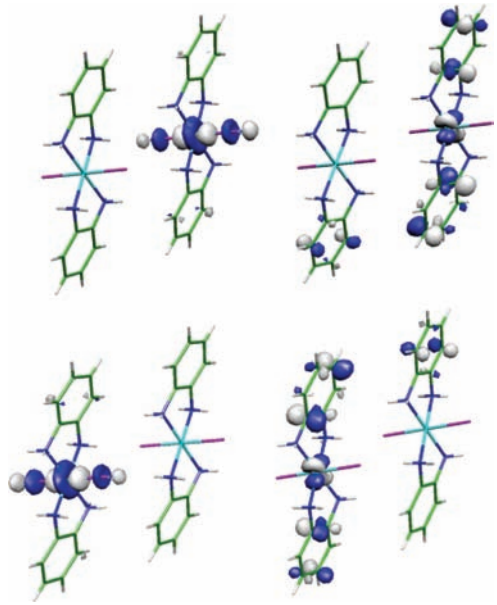

Figure 8. Representation of the molecular orbitals bearing the four unpaired electrons in the model structure corresponding to the type 1 interaction and the broken-symmetry solution.

angle will result in a less efficient exchange pathway. Thus, it is important to keep in mind that the exchange coupling constant through the type 1 interaction is more than twice as antiferromagnetic as through the corresponding type 2 interaction, despite the smaller Ni−Cl···N angle. This is not only due to the presence of a double pathway for the exchange but also due to the role played by the relative orientation of the molecules.

The molecular orbitals bearing the unpaired electrons for the type 1 interaction are represented in Figure 8. These orbitals do not shown any significant contribution of the hydrogen atoms involved in the exchange pathway. Thus, it seems that the role of the hydrogen bonds is just a glue to close up the molecules, but the hydrogen atoms are not relevant from the point of view of their participation in the exchange pathway, as has been noticed previously.[29]

Finally, it is interesting to note that the exchange coupling found in the title compound through the N−H···Cl H bonds is similar to those found in other H-bonded systems with similar weak H-bonds[35−41] but weaker than the ones found in systems with stronger H-bonds.[41−44]

CONCLUSIONS

We have shown that $NiCl_2(opda)_2$ presents very weak antiferromagnetic interactions through two different types of N−H···Cl H-bonds. Since the fit of the magnetic properties gives similar J values for both interactions (J = −1.72(1) cm^{-1} and J' = −0.22(1) cm^{-1}) and the structural parameters do not allow an unambiguous assignation of the exchange parameters to the exchange pathways, we have performed DFT calculations that show values similar to those obtained experimentally (J = −1.39 cm^{-1} and J' = −0.56 cm^{-1}) and allow us to assign the strongest coupling to the double N−H···Cl, type 1, H bond and the weakest coupling to the single N−H···Cl, type 2, H bond.

dx.doi.org/10.1021/ic3007124 | Inorg. Chem. 2012, 51, 5487−5493

■ ASSOCIATED CONTENT

Supporting Information

This material is available free of charge via the Internet at http://pubs.acs.org.

■ AUTHOR INFORMATION

Corresponding Author

*E-mail: rwillett@wsu.edu.

Notes

The authors declare no competing financial interest.

■ ACKNOWLEDGMENTS

The Bruker (Siemens) SMART APEX diffraction facility was established at the University of Idaho with the assistance of the NSF-EPSCoR program and the M. J. Murdock Charitable Trust, Vancouver, WA, USA. R.D.W. appreciates the continuing support of the Department of Chemistry and the College of Science of Washington State University. The assistance of Dr. Karen Maxcy in preparation of the sample is appreciated. The authors acknowledge the European Union for financial support (MAGMANet Network of Excellence), the Spanish Ministerio de Economía y Competitividad (Projects MAT2007-61584, CTQ2011-23862-C02-01, CTQ2011-26507, and Consolider-Ingenio 2010 CSD 2007-00010 in Molecular Nanoscience), and Agència de Gestió d'Ajuts Universitaris i de Recerca (Generalitat de Catalunya) through grant 2005SGR-00036. S.G.C. thanks Ministerio de Educación, Cultura y Deporte for a predoctoral fellowship. The computing resources were generously made available at the Centre de Serveis Científics i Acadèmics de Catalunya (CESCA) through a grant provided by the Direcció General de Recerca and the Universitat de Barcelona.

■ REFERENCES

(1) (a) Yuan, M.; Zhao, F.; Zhang, W.; Wang, Z.-M.; Gao, S. *Inorg. Chem.* **2007**, *46*, 11235. (b) Kubono, K.; Hirayama, N.; Kokusen, H.; Yokoi, K. *Anal. Sci.* **2001**, *17*, 193. (c) El-Shahawi, M. S.; Smith, W. E. *Analyst* **1994**, *119*, 327.

(2) (a) Cutler, A. R.; Dolphin, D. *Can. J. Chem.* **1977**, *55*, 3062. (b) Çolak, A. T.; Tümer, M.; Serin, S. *Trans. Met. Chem.* **2000**, *25*, 200.

(3) (a) Jubb, J.; Larkworthy, L. F.; Oliver, L. F.; Povey, D. C.; Smith, G. W. *J. Chem. Soc., Dalton Trans.* **1991**, 2045. (b) Narayanan, B.; Bhadbhade, M. M. *Acta Crystallogr. C* **1996**, *52*, 3049. (c) Gustafsson, B.; Haakansson, M.; Jagner, S. *Inorg. Chim. Acta* **2005**, *358*, 209. (d) Elder, R. C.; Koran, D.; Mark, H. B., Jr. *Inorg. Chem.* **1974**, *13*, 1644. (e) Russell, J.; Bilich, M.; Olmstead, M. M. *Inorg. Chim. Acta* **2003**, *348*, 212. (f) Qin, B.-H.; Ma, W-Xi.; Lu, L.-D.; Yang, X.-J.; Wang, X. *Acta Crystallogr. E* **2007**, *63*, m2930.

(4) (a) Wang, C. F.; Li, D. P.; Chen, X.; Li, X. M.; Li, Y. Z.; Zuo, J. L.; You, X. Z. *Chem. Commun.* **2009**, 6940. (b) Toftlund, H.; Simonsen, O. *Inorg. Chem.* **1984**, *23*, 4261. (c) Liu, F.; Chen, W *J. Coord. Chem.* **2006**, *59*, 1629. (d) Wang, C. F.; Gu, Z. G.; Lu, X. M.; Zuo, J. L.; You, X. Z. *Inorg. Chem.* **2008**, *47*, 7957. (e) Miao, Z. X.; Li, M. X.; Shao, M.; Liu, H. J. *Inorg. Chem. Commun.* **2007**, *10*, 1117. (f) Mizuta, T.; Miyoshi, K. *Bull. Chem. Soc. Jpn.* **1991**, *64*, 1859. (g) Nayak, M.; Kundu, P.; Lemoine, P.; Koner, R.; Wei, H. H.; Mohanta, S. *Polyhedron* **2006**, *25*, 2007. (h) Coronado, E.; Gómez-García, C. J.; Nuez, A.; Romero, F. M.; Rusanov, E.; Stoeckli-Evans, H. *Inorg. Chem.* **2002**, *41*, 4615. (i) Bellouard, F.; Clemente-León, M.; Coronado, E.; Galán-Mascarós, J. R.; Giménez-Saiz, C.; Gómez-García, C. J.; Woike, T. *Polyhedron* **2001**, *20*, 1615. (j) Bellouard, F.; Clemente-León, M.; Coronado, E.; Galán-Mascarós, J. R.; Gómez-García, C. J.; Romero, F.; Dunbar, K. R. *Eur. J. Inorg. Chem.* **2002**, 1603.

(5) (a) Malkov, A. E.; Aleksandrov, G. G.; Ikorskii, V. N.; Sidorov, A. A.; Fomina, I. G.; Nefedov, S. E.; Novotortsev, V. M.; Eremenko, I. L.; Moiseev, I. I. *Koord. Khim.* **2001**, *27*, 677. (b) Ariyananda, W. G. P.; Norman, R. E. *Acta Crystallogr. E* **2005**, *61*, m187. (c) Supriya, S.; Das, S. K. *Inorg. Chem. Commun.* **2009**, *12*, 364. (d) Chen, Z. L.; Zhang, Y. Z.; Liang, F. P. *Acta Crystallogr. E* **2006**, *62*, m1296. (e) Elder, R. C.; Koran, D.; Mark, H. B., Jr. *Inorg. Chem.* **1974**, *13*, 1644. (f) Li, J. P.; Li, L. H.; Wu, L. M.; Chen, L. *Inorg. Chem.* **2009**, *48*, 1260.

(6) Maxcy, K. R.; Smith, R.; Willett, R. D.; Vij, A. *Acta Crystallogr. C* **2000**, *56*, e454.

(7) (a) Balzani, V.; Gedi, A.; Raymo, F. M.; Stoddart, J. F. *Angew. Chem., Int. Ed.* **2000**, *39*, 3348. (b) Inorganic Crystal Engineering, Dalton Discussion No. 3, *J. Chem. Soc., Dalton Trans.* **2000**, 3705. (c) Steiner, T. *Angew. Chem., Int. Ed.* **2002**, *41*, 48.

(8) (a) Ruiz, E.; Alemany, P.; Alvarez, S.; Cano, J. *J. Am. Chem. Soc.* **1997**, *119*, 1297. (b) Ruiz, E.; Alvarez, S.; Rodríguez-Fortea, A.; Alemany, P.; Pouillon, Y.; Massobrio, C. In *Magnetism: Molecules to Materials*; Miller, J. S., Drillon, M., Eds.; Wiley-VCH: Weinheim, 2001; Vol. 2, p 227.

(9) Ruiz, E. *Struct. Bonding (Berlin)* **2004**, *113*, 71.

(10) *SMART*, v. 5.632; Bruker AXS: Madison, WI, 2005.

(11) *SAINTPlus, Data Reduction and Correction Program*, v. 7.23a; Bruker AXS: Madison, WI, 2004.

(12) *SADABS, an Empirical Absorption Correction Program*, v.2007/4; Bruker AXS Inc.: Madison, WI, 2007.

(13) Sheldrick, G. M. *SHELXTL, Structure Determination Software Suite*, v. 6.14; Bruker AXS Inc.: Madison, WI, 2004.

(14) Ruiz, E.; Alvarez, S.; Cano, J.; Polo, V. *J. Chem. Phys.* **2005**, *123*, 164110.

(15) Ruiz, E.; Cano, J.; Alvarez, S.; Alemany, P. *J. Comput. Chem.* **1999**, *20*, 1391.

(16) Ruiz, E.; Rodríguez-Fortea, A.; Cano, J.; Alvarez, S.; Alemany, P. *J. Comput. Chem.* **2003**, *24*, 982.

(17) Ruiz, E.; Rodríguez-Fortea, A.; Tercero, J.; Cauchy, T.; Massobrio, C. *J. Chem. Phys.* **2005**, *123*, 074102.

(18) Noodleman, L.; Case, D. A. *Adv. Inorg. Chem.* **1992**, *38*, 423.

(19) Becke, A. D. *J. Chem. Phys.* **1993**, *7*, 5648.

(20) Frisch, M. J.; Trucks, G. W.; Schlegel, H. B.; Scuseria, G. E.; Robb, M. A.; Cheeseman, J. R.; Montgomery, J. A.; Vreven, T.; Kudin, K. N.; Burant, J. C.; Millam, J. M.; Iyengar, S. S.; Tomasi, J.; Barone, V.; Mennucci, B.; Cossi, M.; Scalmani, G.; Rega, N.; Petersson, G. A.; Nakatsuji, H.; Hada, M.; Ehara, M.; Toyota, K.; Fukuda, R.; Hasegawa, J.; Ishida, H.; Nakajima, T.; Honda, Y.; Kitao, O.; Nakai, H.; Klene, M.; Li, X.; Knox, J. E.; Hratchian, H. P.; Cross, J. B.; Adamo, C.; Jaramillo, J.; Gomperts, R.; Stratmann, R. E.; Yazyev, O.; Austin, A. J.; Cammi, R.; Pomelli, C.; Ochterski, J.; Ayala, P. Y.; Morokuma, K.; Voth, G. A.; Salvador, P.; Dannenberg, J. J.; Zakrzewski, V. G.; Dapprich, S.; Daniels, A. D.; Strain, M. C.; Farkas, O.; Malick, D. K.; Rabuck, A. D.; Raghavachari, K.; Foresman, J. B.; Ortiz, J. V.; Cui, Q.; Baboul, A. G.; Clifford, S.; Cioslowski, J.; Stefanov, B. B.; Liu, G.; Liashenko, A.; Piskorz, P.; Komaromi, I.; Martin, R. L.; Fox, D. J.; Keith, T.; Al-Laham, M. A.; Peng, C. Y.; Nanayakkara, A.; Challacombe, M.; Gill, P. M. W.; Johnson, B.; Chen, W.; Wong, M. W.; Gonzalez, C.; Pople, J. A. *Gaussian03*; Gaussian, Inc: Pittsburgh, PA, 2003.

(21) Becke, A. D. *Phys. Rev. A* **1988**, *38*, 3098.

(22) Lee, C.; Yang, W.; Parr, R. G. *Phys. Rev. B* **1988**, *37*, 785.

(23) Schaefer, A.; Huber, C.; Ahlrichs, R. *J. Chem. Phys.* **1994**, *100*, 5829.

(24) (a) Weng, C. Y. Ph.D. Thesis, Carnegie-Mellon University, 1968. (b) Blöte, H. W. *J. Phys. B* **1975**, *79*, 427. (c) de Neef, T. *Phys. Rev. B* **1976**, *13*, 4141.

(25) Lines, M. E. *J. Phys. Chem. Solids* **1970**, *31*, 101.

(26) O'Connor, C. J. *Prog. Inorg. Chem.* **1982**, *29*, 203.

(27) Boca, R. *Coord. Chem. Rev.* **2004**, *248*, 757.

(28) Borrás-Almenar, J. J.; Coronado, E.; Curely, J.; Georges, R. *Inorg. Chem.* **1995**, *34*, 2699.

(29) Desplanches, C.; Ruiz, E.; Rodríguez-Fortea, A.; Alvarez, S. *J. Am. Chem. Soc.* **2002**, *124*, 5197.

(30) Gómez-Coca, S.; Ruiz, E. *Dalton Trans.* **2012**, *41*, 2659.

(31) Shapiro, A.; Landee, C. P.; Turnbull, M. M.; Jornet, J.; Deumal, M.; Novoa, J. J.; Robb, M. A.; Lewis, W. *J. Am. Chem. Soc.* **2007**, *129*, 952.
(32) Wernsdorfer, W.; Aliaga-Alcalde, N.; Hendrickson, D. N.; Christou, G. *Nature* **2002**, *416*, 406.
(33) Cano, J.; Ruiz, E.; Alvarez, S.; Verdaguer, M. *Comments Inorg. Chem.* **1998**, *20*, 27.
(34) Ruiz, E.; Cirera, J.; Alvarez, S. *Coord. Chem. Rev.* **2005**, *249*, 2649.
(35) Arulsamy, N.; Glerup, J.; Hodgson, D. J. *Inorg. Chem.* **1994**, *33*, 2066.
(36) Nieuwpoort, G.; Verschoor, G. C.; Reedijk, J. *J. Chem. Soc., Dalton Trans.* **1983**, 531.
(37) Masi, D.; Mealli, C.; Sabat, M.; Sabatini, A.; Vacca, A.; Zanobini, F. *Helv. Chim. Acta* **1984**, *67*, 1818.
(38) Klein, C. L.; Majeste, R. J.; Trefonas, L. M.; O'Connor, C. J. *Inorg. Chem.* **1982**, *21*, 1891.
(39) Estes, W. E.; Hatfield, W. E. *Inorg. Chem.* **1978**, *17*, 3226.
(40) Ueki, T.; Ashida, T.; Sasada, Y.; Kakudo, M. *Acta Crystallogr. B* **1969**, *25*, 328.
(41) Plass, W.; Pohlmann, A.; Rautengarten, J. *Angew. Chem., Int. Ed.* **2001**, *40*, 4207.
(42) Bertrand, J. A.; Black, T. D.; Eller, P. G.; Helm, F. T.; Mahmood, R. *Inorg. Chem.* **1976**, *15*, 2965.
(43) Bertrand, J. A.; Fujita, E.; Vanderveer, D. G. *Inorg. Chem.* **1980**, *19*, 2022.
(44) Muhonen, H. *Inorg. Chem.* **1986**, *25*, 4692.